# Differential Proteomic Analysis Using iTRAQ Reveals Alterations in Hull Development in Rice (*Oryza sativa* L.)

Shuzhen Wang[1,2,3☿], Wenyue Chen[1☿], Wenfei Xiao[1], Changdeng Yang[2], Ya Xin[1], Jieren Qiu[1], Weimin Hu[3], Wu Ying[1], Yaping Fu[2], Jianxin Tong[1], Guocheng Hu[2], Zhongzhong Chen[1], Xianping Fang[1], Hong Yu[1], Wenguo Lai[1], Songlin Ruan[1]*, Huasheng Ma[1]*

1 Laboratory of Plant Molecular Biology & Proteomics, Institute of Biotechnology, Hangzhou Academy of Agricultural Sciences, Hangzhou 310024, China, 2 State Key Laboratory of Rice Biology, China National Rice Research Institute, Hangzhou 310006, China, 3 Department of Agronomy, College of Agriculture and Biotechnology, Zhejiang University, Hangzhou 310012, China

☿ These authors contributed equally to this work.
* ruansl1@hotmail.com (SR); hzhsma@163.com (HM)

## Abstract

Rice hull, the outer cover of the rice grain, determines grain shape and size. Changes in the rice hull proteome in different growth stages may reflect the underlying mechanisms involved in grain development. To better understand these changes, isobaric tags for relative and absolute quantitative (iTRAQ) MS/MS was used to detect statistically significant changes in the rice hull proteome in the booting, flowering, and milk-ripe growth stages. Differentially expressed proteins were analyzed to predict their potential functions during development. Gene ontology (GO) terms and pathways were used to evaluate the biological mechanisms involved in rice hull at the three growth stages. In total, 5,268 proteins were detected and characterized, of which 563 were differentially expressed across the development stages. The results showed that the flowering and milk-ripe stage proteomes were more similar to each other ($r$=0.61) than either was to the booting stage proteome. A GO enrichment analysis of the differentially expressed proteins was used to predict their roles during rice hull development. The potential functions of 25 significantly differentially expressed proteins were used to evaluate their possible roles at various growth stages. Among these proteins, an unannotated protein (Q7X8A1) was found to be overexpressed especially in the flowering stage, while a putative uncharacterized protein (B8BF94) and an aldehyde dehydrogenase (Q9FPK6) were overexpressed only in the milk-ripe stage. Pathways regulated by differentially expressed proteins were also analyzed. Magnesium-protoporphyrin IX monomethyl ester [oxidative] cyclase (Q9SDJ2), and two magnesium-chelatase subunits, ChlD (Q6ATS0), and ChlI (Q53RM0), were associated with chlorophyll biosynthesis at different developmental stages. The expression of Q9SDJ2 in the flowering and milk-ripe stages was validated by qRT-PCR. The 25 candidate proteins may be pivotal markers for controlling rice hull development at various growth stages and chlorophyll biosynthesis pathway related proteins, especially magnesium-protoporphyrin IX monomethyl

ester [oxidative] cyclase (Q9SDJ2), may provide new insights into the molecular mechanisms of rice hull development and chlorophyll associated regulation.

## Introduction

Rice (*Oryza sativa* L.) supports nearly half the world population and is one of the world's most important grain crops [1–4]. The mature rice seed consists of caryopsis and hull. The rice caryopsis contains the caryopsis coat, aleurone, embryo and starchy endosperm. The aleurone layer is the outermost layer of the endosperm, followed by the inner starchy endosperm [5]. The embryo consists of the scutellum, embryonic axis and various sheathing structures. The starchy endosperm, accounting for over 80% of the caryopsis, contains parenchyma cells filled with reserves [6]. The rice hull (husk), the outer cover of the rice grain, is an important floral organ comprised of lemma and palea. The lemma covers two-thirds of the seed, while the palea is the lining that hugs the seed. The hull is indigestible because of the presence of opaline silica (a hydrated form of silica) and lignin, a complex component that helps to hydrate the rice grain. Rice hull not only acts as a mechanical barrier to prevent damage and maintain humidity for the developing seed, but is also a critical factor that affects yield and milling quality of the grain in terms of its volume, shape, and size [7–12].

Genetic studies and gene cloning have helped understand the functions of the large numbers of genes involved in rice hull development. For example, a rice mutant with twisted hull (*twh*) derived from a breeding population of rice was reported to exhibit reduced grain weight compared with the wild type parent [13]. Similarly, a rice floral organ mutant (*bh1*) has a beak-shaped hull, which was found to have a negative effect on grain yield [14]. The stunted lemma palea 1 rice mutant (*slp1*) displays severely degenerated lemmas/paleae, and *SLP1* was reported to be localized in a 46.4-kb genomic region that contained three putative genes, *OsSPL16*, *OsMADS45*, and *OsMADS37* [15]. A palea formation controlling gene, depressed palea 1 (*dp1*), encodes a nuclear-localized AT-hook DNA-binding protein that causes a primary defect in the main structure of the palea, which is required for palea formation and floral organ number control [16]. The rice MADS-box factor (*OsMADS1*) is an early-acting regulator of inner floral organs that controls the differentiation of specific cell types in the lemma and palea [17]. Li and coworkers found that *TH1* accumulated mainly in young inflorescence and was important in controlling lemma and palea development in rice [8]. Other genes that have been reported to be associated with rice hull development include frizzy panicle (*FZP*) [18], abnormal hull (*ah*) [19], sterile lemma (*G1*) [20], and elongated empty glume (*ELE*) [21]. Nevertheless, the genetic regulation of rice hull development has not yet been established. Systematic genome-wide analysis may provide further insights into the molecular genetic mechanisms associated with rice hull development.

Microarray technologies are useful for high-throughput gene expression analysis [22]. However, mRNA expression levels may not translate precisely into protein function and, therefore, mRNA profiling may not fully characterize the functional proteome. Proteomic research areas are currently mainly focused on abiotic stress and biotic stress in rice [23], the lack of a validated, high-throughput, quantitative functional proteomics platform for rice hull remains a major barrier to the identification of the underlying molecular mechanisms associated with its development.

The isobaric tags for relative and absolute quantification (iTRAQ) method has been developed for the simultaneous quantitative comparison and analysis of protein expression profiles

of multiple samples [24–26]. Quantitative proteomic mass spectrometry methodologies can be classified into three categories: label-free (non-labeled), gel-based, and label-based. The labeled iTRAQ technique, which uses isotopic label-based protocols, yields very small coefficients of variation in quantitative measurements and is considered one of the most robust techniques for differential quantitative proteomic analyses [27, 28]. In the present study, we applied label-based iTRAQ to analyze quantitatively the alternations of the hull proteome in the booting stage, flowering stage, and milk-ripe stage of hull development. The aim was to identify differentially expressed proteins of the rice hull at various growth stages. The results provide a global insight into changes of the rice hull proteome during development.

## Materials and Methods

### Sample collection

A tested super-hybrid rice variety (*O. sativa* cv. LYP9) was supplied by the Wu Wang Nong Seed Group (Hangzhou, Zhejiang Province, China). Four replicates of 100 seeds were soaked in water for 24 h at 30°C to accelerate hydration and then transferred to germination boxes (18 cm × 13 cm × 10 cm) containing two layers of blotters moistened with distilled water. The seeds were germinated in a chamber for 1 d at 30°C to accelerate germination. Germinating seeds were sown in paddy soil on 14 June 2011. The rice plants started heading on 10 September 2011. Fresh hull samples at three different developmental stages, booting stage (PK1), flowering stage (PK2), and milk-ripe stage (PK3), were collected during heading and stored at -80°C until protein preparation.

### Protein preparation

One gram fresh weight of hulls was ground in liquid nitrogen and suspended in 5 ml of 10% (w/v) trichloroacetic acid in acetone with 0.07% (w/v) β-mercaptoethanol at -20°C for 1 h, followed by centrifugation for 15 min at 35,000 × *g*. The pellets were resuspended in acetone with 0.07% (w/v) β-mercaptoethanol and incubated at -20°C for 1 h, and then centrifuged for 15 min at 4°C. This step was repeated three times, after which the pellets were lyophilized. The crude protein power was solubilized in lysis buffer (8 M urea, 2 M thiourea, 4% CHAPS, 0.5% ampholine (pH 3–10), 50 mM DTT, and 1 mM PMSF) for 1 h at room temperature, followed by centrifugation for 15 min at 15,000 × *g*. The supernatant was collected in a 1.5-ml tube, and a 40-μl sample was taken to determine the protein concentration using the Bradford assay with bovine serum albumin as the standard.

### Protein digestion and iTRAQ labeling

Protein digestion was performed according to the FASP procedure [29] and the resulting peptide mixture was labeled using the 4-plex iTRAQ reagent according to the manufacturer's instructions (Applied Biosystems, Boston, MA, USA). Briefly, 200 μg of protein for each sample was incorporated into 30 μl STD buffer (4% SDS, 100 mM DTT, 150 mM Tris-HCl pH 8.0). The detergent DTT and other low-molecular-weight components were removed using UA buffer (8 M Urea, 150 mM Tris-HCl pH 8.0) by repeat ultrafiltration (Microcon units, 30 kD). Then 100 μl 0.05 M iodoacetamide in UA buffer was added to block reduced cysteine residues and the samples were incubated for 20 min in the dark. The filters were washed three times with 100 μl UA buffer, and then twice with 100 μl DS buffer (50 mM triethylammonium-bicarbonate at pH 8.5). Finally, the protein suspensions were digested with 2 μg trypsin (Promega, Madison, WI, USA) in 40 μl DS buffer overnight at 37°C, and the resulting peptides were collected as a filtrate. The peptide content was estimated by UV light spectral density at

280 nm using an extinctions coefficient of 1.1 of 0.1% (g/l) solution that was calculated based on the frequency of tryptophan and tyrosine in vertebrate proteins.

For labeling, each iTRAQ reagent was dissolved in 70 μl of ethanol and added to the respective peptide mixture. The PK1 sample was divided into two parts that were labeled as (PK1)-114 and (PK1)-115. The sample that was labeled as (PK1)-114 was served as the control. The remaining samples were labeled as (PK2)-116 and (PK3)-117. All labeled samples were multiplexed and vacuum dried.

## Peptide fractionation with strong cation exchange (SCX) chromatography

The iTRAQ labeled peptides were fractionated by SCX chromatography using an AKTA Purifier system (GE Healthcare, London, UK). The dried peptide mixture was reconstituted and acidified with 2 ml buffer A (10 mM $KH_2PO_4$ in 25% of acetonitrile, pH 2.7) and loaded onto a PolySulfoethyl 4.6 x 100 mm column (5 μm, 200 Å, PolyLC Inc, Colombia, MD, USA). The peptides were eluted at a flow rate of 1 ml/min with a buffer B (500 mM KCl, 10 mM $KH_2PO_4$ in 25% acetonitrile, pH 2.7) gradient of 0%–10% for 2 min, 10%–20% for 25 min, 20%–45% for 5 min, and 50%–100% for 5 min. The elution was monitored by absorbance at 214 nm, and fractions were collected every 1 min. The collected fractions (about 30 fractions) were finally combined into 10 pools and desalted on C18 Cartridges (Empore SPE Cartridges C18 (standard density), bed I.D. 7 mm, volume 3 ml, Sigma, Santa Clara, CA, USA). Each fraction was concentrated by vacuum centrifugation and reconstituted in 40 μl of 0.1% (v/v) trifluoroacetic acid. All samples were stored at -80°C until analysis by liquid chromatography with tandem mass spectrometry (LC-MS/MS).

## LC-MS/MS analysis

From each fraction, 10 μg was trapped on a precolumn (200 μm x 0.5 mm) and then eluted on an analytical column (75 μm x 15 cm) for separation. Both columns were packed with Reprosil-Pur (RP) C18-AQ 3 μm 120Å phase (Eksigent, Dublin, CA, USA). The RP mobile phase A was 98% water (with 2% acetonitrile and 0.1% formic acid) while RP mobile phase B was 98% acetonitrile (with 2% $H_2O$ and 0.1% formic acid). The peptides were separated over 90 min using a linear gradient of 12%–30% of RP mobile B at a flow rate of 300 nl/min. The MS analysis was performed using a 5600 TripleTOF analyzer (QqTOF; AB SCIEX, Boston, MA, USA) in Information Dependent Mode. Precursor ions were selected across the mass range of 350–1250 m/z using 250 ms accumulation time per spectrum. A maximum of 30 precursors per cycle from each MS spectrum were selected for MS/MS analyses with 100 ms minimum accumulation time for each precursor and dynamic exclusion for 25 s. The MS/MS spectra were recorded in high sensitivity mode with rolling collision energy on and iTRAQ reagent collision energy adjustment on.

## Protein identification and relative quantitation criteria

Protein identification and relative iTRAQ quantification were performed with the Paragon algorithm [30] in the ProteinPilot Software 4.2 (AB SCIEX, Boston, MA), and the results were further processed using the Pro Group algorithm, where isoform-specific quantification was adopted to trace the differences between the expressions of various isoforms. Quantitative ratio of reporter ions, calculated by comparing the peak areas of each of these reporter ions in the mass spectrum, was used to evaluate the expression change of the protein in different samples. Normalization has been done during the quantification to correct experimental bias. Strict criteria were imposed to reduce the numbers of false positive expression changes. To accept

proteins as showing differential expression between the different stages, we used the following criteria: 1) Proteins must have been identified in all four iTRAQ preparations; 2) Proteins must have been identified with greater than 95% confidence; 3) Proteins with 20% increase or decrease in replicated experiments (iTRAQ ratios (PK1)-115:(PK1)-114 <0.8 or >1.2) were excluded; and 4) Proteins with a ratio fold change >2 or <0.5 in expression (iTRAQ ratios (PK2)-116:(PK1)-114 or (PK3)-117:(PK1)-114 of >2 or <0.5) and a significant p-value (p <0.05) were considered to be differentially expressed.

## Protein mass spectrum hierarchical cluster analysis and statistical analysis

We selected 563 proteins from the 5,268 identified proteins for further analysis and the $\log_2$ ratios were normalized globally for each sample. To cluster the rice husk proteins of the three growth stages, we used Ward's method, a hierarchical technique. Function heatmap.2 from the R package gplots was used to produce the graphical display of the dendrogram [31]. Pearson's correlation coefficient and scatter plots were used to estimate the relationship between two random samples at various growth stages. Lowess was used to smooth the scatter plots by locally weighted regression. All the statistical analyses were performed in the R environment, using several CRAN packages (http://cran.r-project.org/).

## Gene ontology and pathway analysis

Gene ontology (GO) [32], UniProt [33], and GOEAST [34] were used to annotate the proteins under the biological process, molecular function, and cellular component GO categories in the booting, flowering, and milk-ripe stages of rice hull development. Rice gene annotations were taken from the Rice Annotation Project Database (RAP-DB) [35] and the Michigan State University (MSU) Rice Genome Annotation [36] website. Circos diagrams [37] were also used to analysis the differences at various growth stages. Proteins that were differentially expressed in the booting stage were analyzed using UniPathway [38] to identify molecular pathways that may be different in this growth stage compared with the other two stages.

## Expression validation by quantitative RT-PCR

Quantitative RT-PCR (qRT-PCR) assays were performed to validate the different expression levels of differentially expressed chlorophyll biosynthesis related proteins in the booting, flowering and milk-ripe growth stages. Relative gene expression levels were quantified based on the cycle threshold (Ct) values and normalized to the reference gene Actin (GenBank: AY212324). Each sample was repeated three times and the gene expression levels were calculated by the $2^{-\Delta\Delta Ct}$ method.

## Results

### Phenotype of rice hull at various growth stages

Rice hull samples were collected at three stages of husk development (Fig 1). The samples collected at the earliest stage, the booting stage, were characterized by swelling of the leaf sheath and elongated internodes. The samples collected at the flowering stage were selected between the opening and closing of the rice flower. The milk-ripe stage samples exhibited starch grains developing in the kernels that were soft and in the interior of the kernel.
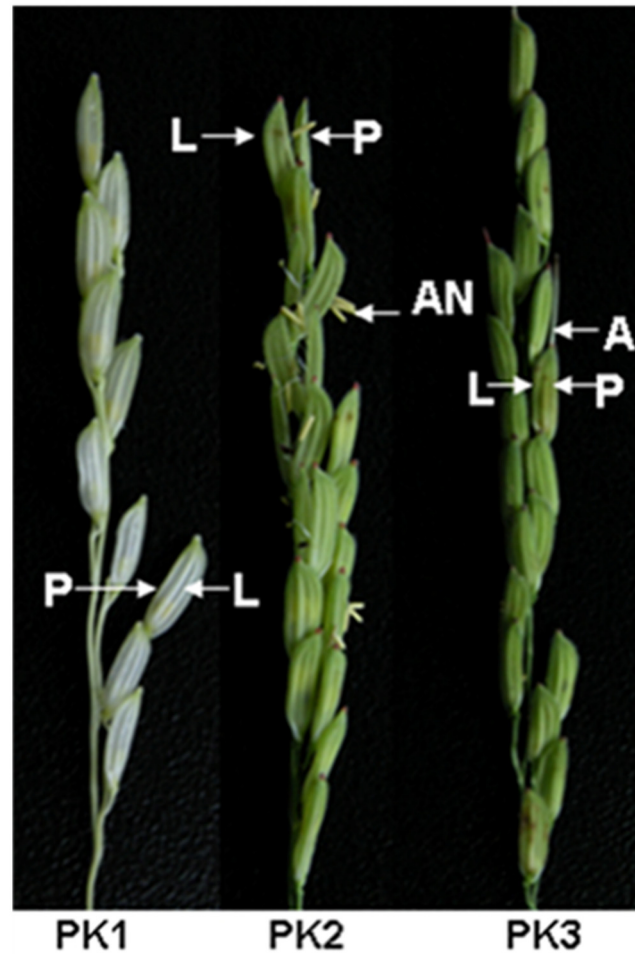
**Fig 1. Phenotype of rice hull in three growth stages.** A, awn; AN, anther; L, lemma; P, palea; PK1, booting stage; PK2, flowering stage; PK3, milk-ripe stage.

doi:10.1371/journal.pone.0133696.g001

## Protein identification and relative expression

Overall, we identified 5268 distinct proteins that had an estimated global False Discovery Rate (FDR) of <0.01. Only proteins that were identified with ≥95% confidence were considered. Among the 5,268 proteins, 563 differentially expressed proteins were identified for further analysis (S1 Table). Compared with their expressions in the booting stage, 235 proteins were upregulated and 326 were downregulated in the flowering stage, and 221 proteins were upregulated and 342 were downregulated in the milk-ripe stage.

## Quantitative comparison of protein expression in the three developmental stages

To investigate the expression levels in the rice hull proteomes at various growth stages, we used Ward's method to perform unsupervised hierarchical clustering analysis of the 563 differentially expressed proteins. The samples were clustered based on the overall similarity in their protein expression patterns and the relationships were summarized in a dendrogram (Fig 2A). Results showed that the protein expression patterns in the flowering and milk-ripe stage
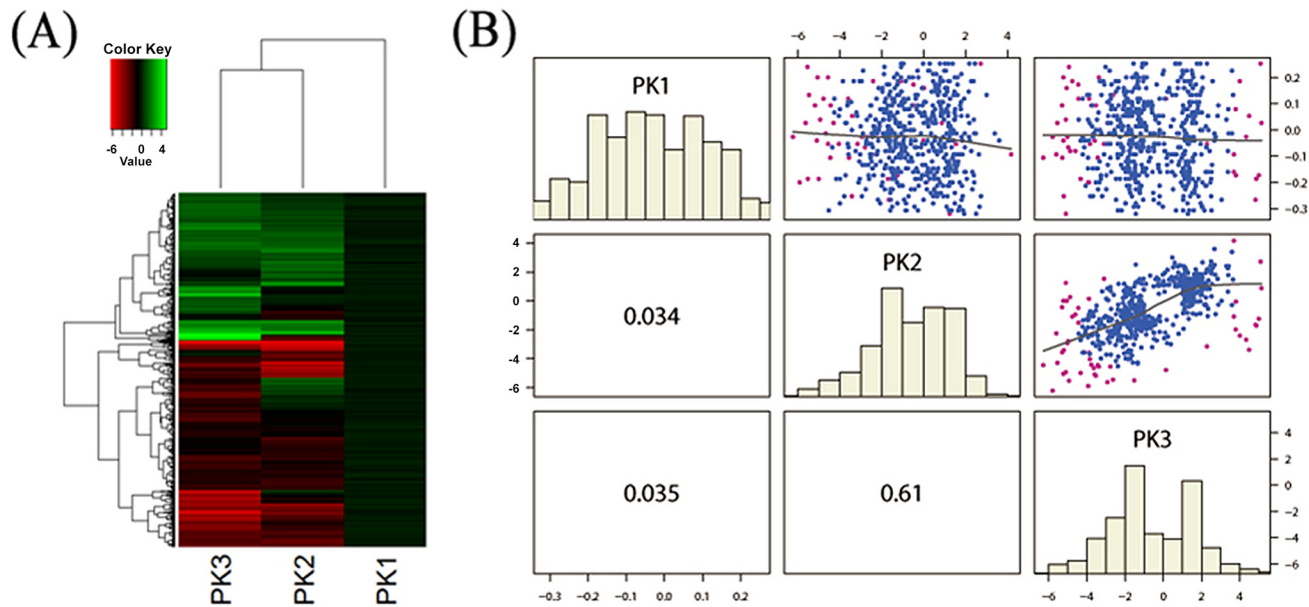
Fig 2. Quantitative comparison of protein expression in the three developmental stages. (A) Hierarchical clustering analysis of protein expression in three growth stages of rice hull. (B) Protein expression correlations in three growth stages of rice hull. PK1, booting stage; PK2, flowering stage; PK3, milk-ripe stage.

proteomes were more similar to each other than either was to the protein expression patterns in the booting stage proteome. In both the flowering and milk-ripe stages the protein expression patterns had very high correlation coefficients ($r = 0.61$), while the correlation coefficient between the flowering or milk-ripe stages and the booting stage were lower ($r = 0.034$ and $r = 0.035$, respectively) (Fig 2B).

## Overall gene ontology analysis

To obtain a global picture of the proteomic changes during rice hull development, the differentially expressed proteins were annotated with GO terms and a GO functional analysis was performed. We found that that 27 biological process terms, four molecular function terms, and 12 cellular component terms were statistically enriched in the booting stage. In the flowering stage, 38 biological process terms, five molecular function terms, and 17 cellular component terms were statistically enriched; while in the milk-ripe stage, 15 biological process terms, nine molecular function terms, and 46 cellular component terms were statistically enriched (Fig 3, S2 Table). The numbers of GO terms in the three categories were more similar in the booting and flowering stages than either was in the milk-ripe stage. Compared with cellular component terms (S1 Fig) and biological process terms (S2 Fig), fewer significant molecular function terms were involved and are more likely to characterize the differentially expressed proteins in the booting, flowering and milk-ripe growth stages.

## Molecular function analysis

Nine highly enriched molecular function GO terms were associated with all three development stages (Fig 4). Catalytic activity, oxidoreductase activity, and cofactor binding were common to rice hull development in the three growth stages, although the numbers of proteins annotated with these terms decreased in the flowering stage and increased in the milk-ripe stage. Proteins
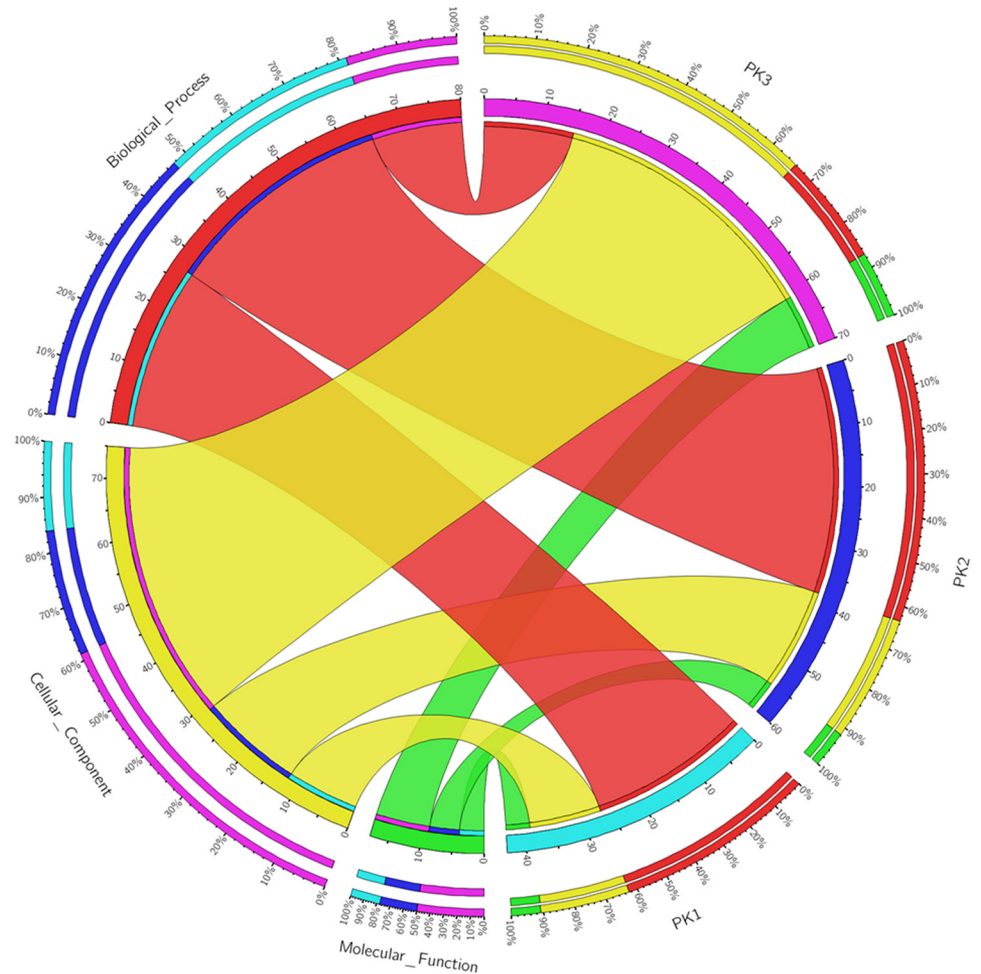
**Fig 3. Gene ontology analysis of differentially expressed proteins in three growth stages of rice hull.**
PK1, booting stage; PK2, flowering stage; PK3, milk-ripe stage.

annotated as coenzyme binding (GO:0050662) were present in the booting stage (P = 0.0756) and milk-ripe stage (P = 0.0164), while proteins annotated as oxidoreductase activity, acting on the aldehyde or oxo group of donors, NAD or NADP as acceptor (GO:0016620), and oxidoreductase activity, acting on the aldehyde or oxo group of donors (GO:0016903) were found in the flowering and milk-ripe stages. The molecular function terms were also compared in the three development stages (Table 1). Overall 333, 93, and 126 proteins involved in catalytic activity were identified in the booting, flowering, and milk-ripe stages, respectively. The numbers of proteins related to oxidoreductase activity and cofactor binding followed the same trend at various growth stages; i.e., highest in the booting stage and lower in the other two stages. Twenty-five proteins annotated with five GO terms (GO:0016620, GO:0016903, GO:0008483, GO:0016769, and GO:0050660) were selected to evaluate the heterogeneity of the rice hull proteome at different growth stages. Among the proteins annotated with the two oxidoreductase activity related terms (GO:0016620 and GO:0016903), five proteins (glyceraldehyde-3-phosphate dehydrogenase 3, cytosolic (GAPC3; Q6K5G8); glyceraldehyde-3-phosphate dehydrogenase (Q8S4Y9); putative cytosolic aldehyde dehydrogenase (Q69XE0); aldehyde dehydrogenase ALDH2b (Aldh2b; Q9FRX7); and putative uncharacterized protein (B8AIJ7)) were common to the flowering and milk-ripe stages; one protein (Q7X8A1) was unique to the flowering stage,
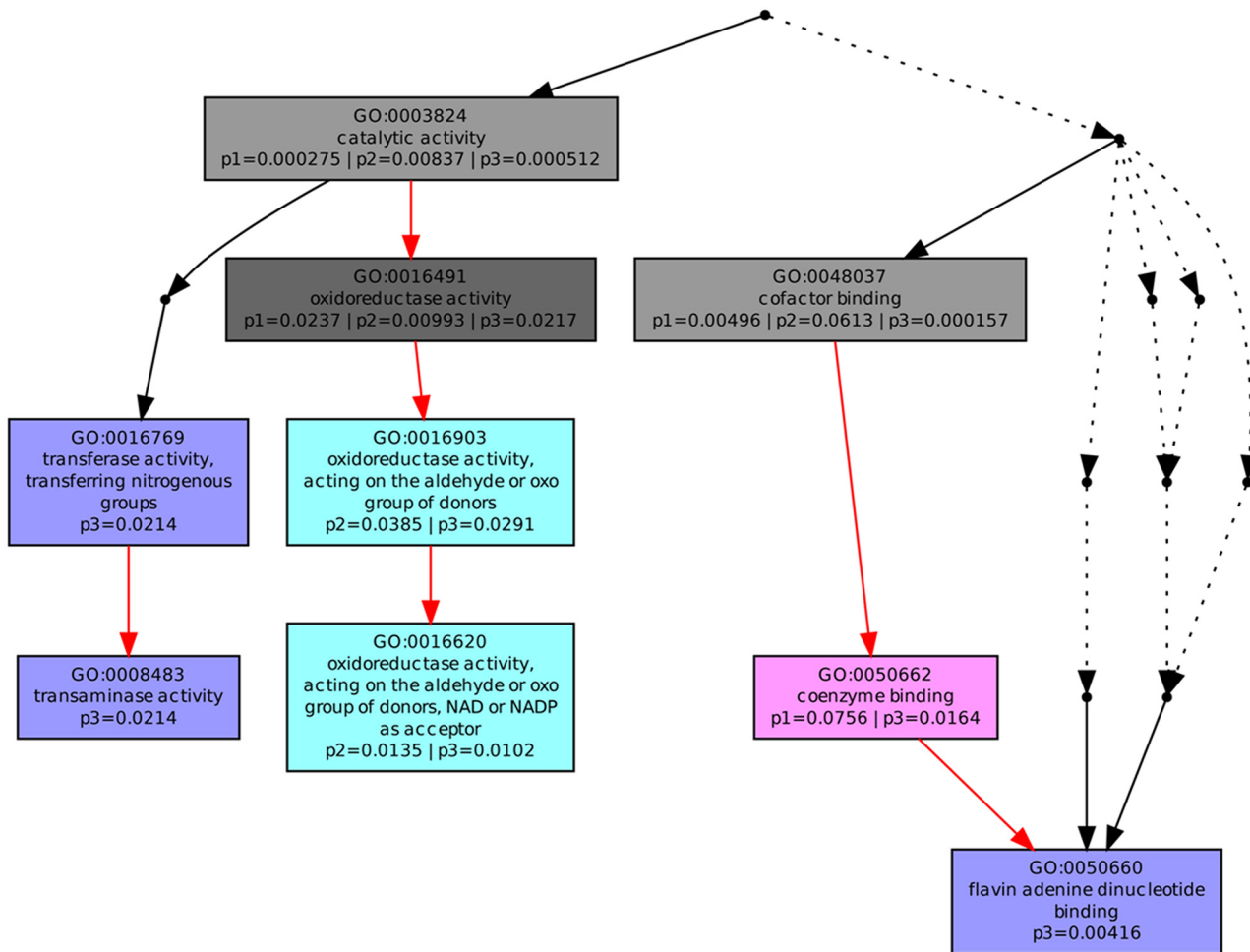
**Fig 4. Molecular function analysis of differentially expressed proteins in three growth stages of rice hull.** P1, booting stage; P2, flowering stage; P3, milk-ripe stage.

doi:10.1371/journal.pone.0133696.g004

and two proteins (B8BF94 and Aldehyde dehydrogenase (ALDH; Q9FPK6)) were found only in the milk-ripe stage. Seventeen proteins unique to the milk-ripe stage were related to transaminase activity (GO:0008483), transferase activity, transferring nitrogenous groups (GO:0016769), and flavin adenine dinucleotide binding (GO:0050660). Seven of the proteins (alanine aminotransferase (Q9S768); aspartate aminotransferase (Q0JJ47); putative acetylornithine aminotransferase (Q688Q8); Q94EG1; aspartate aminotransferase (Q6KAJ2); B8ANL7, and Q5N9Z8) were annotated with two of the terms (GO:0008483 and GO:0016769), while the other ten proteins (A2WTU1; B8AYF2; B7E6V7; Q0DWI9; thioredoxin reductase (B8B5I4); Q0D8R4; putative ferredoxin-NADP(H) oxidoreductase (Q6ZFJ3); probable D-2-hydroxyglutarate dehydrogenase, mitochondrial (D2HGDH; Q7XI14); acetolactate synthase (ALS; A5X300); and putative CPRD2 (Q5Z952) were annotated with GO:0050660.

## Pathway analysis and qRT-PCR validation

The iTRAQ results were also evaluated using UniPathway. Twenty-six proteins in the booting stage samples were assigned to 19 pathways, including sucrose biosynthesis, glycolysis, chlorophyll biosynthesis, and oxylipin biosynthesis. The regulation of proteins corresponding to the

**Table 1. Molecular function of related proteins in three growth stages of rice hull.**

| Molecular Function (GO ID) | Term | Protein Number | | | | | P-value |
|---|---|---|---|---|---|---|---|
| | | | Shared[a] | Unique/Total | | | |
| | | | | PK1[b] | PK2[b] | PK3[b] | |
| GO:0003824 | catalytic activity | | 57 | 171/333 | 0/93 | 0/126 | 0.003053581 |
| GO:0016491 | oxidoreductase activity | | 22 | 43/94 | 0/33 | 0/40 | 0.018451297 |
| GO:0048037 | cofactor binding | | 12 | 18/50 | 0/17 | 0/27 | 0.022130506 |
| GO:0050662 | coenzyme binding | | 18 | 17/35 | - | 0/18 | 0.046026777 |
| GO:0016620 | oxidoreductase activity, acting on the aldehyde or oxo group of donors, NAD or NADP as acceptor | | 5 | - | 1/6 | 2/7 | 0.011866133 |
| GO:0016903 | oxidoreductase activity, acting on the aldehyde or oxo group of donors | | 5 | - | 1/6 | 2/7 | 0.03380623 |
| GO:0008483 | transaminase activity | | 0 | - | - | 7/7 | 0.021352469 |
| GO:0016769 | transferase activity, transferring nitrogenous groups | | 0 | - | - | 7/7 | 0.021352469 |
| GO:0050660 | flavin adenine dinucleotide binding | | 0 | - | - | 10/10 | 0.00416116 |

[a]Shared indicates proteins with a shared molecular function in the existed significant molecular function of the three growth stages.
[b]PK1, booting stage; PK2, flowering stage; PK3, milk-ripe stage.

doi:10.1371/journal.pone.0133696.t001

related pathways varied in the flowering and milk-ripe stages. Compared with the booting stage, six proteins were up-regulated and six were down-regulated in the flowering stage, while 11 proteins were up-regulated (Table 2) and 10 were down-regulated in the milk-ripe stage (Table 3). The expressions of GAPC3 (Q6K5G8) in the glycolysis pathway, phenylalanine

**Table 2. Pathway analysis of differentially upregulated expressed proteins in the flowering and milk-ripe stages compared with the booting stage.**

| Pathway | Control (PK1)[a] | Upregulated (PK2)[a] | Upregulated (PK3)[a] |
|---|---|---|---|
| L-methionine biosynthesis via salvage pathway | F4MG97 | F4MG97 | |
| trans-cinnamate biosynthesis | Q0DZE3;B7EFQ4;Q6K6Q1 | B7EFQ4 | B7EFQ4;Q6K6Q1 |
| chlorophyll biosynthesis (light-independent) | Q9SDJ2 | Q9SDJ2 | |
| chlorophyll biosynthesis | Q6ATS0;Q53RM0 | | |
| Pyruvate fermentation to lactate | Q0E4Q5 | | |
| Oxylipin biosynthesis | A2XL22 | | A2XL22 |
| sucrose biosynthesis | Q0JGK4 | Q0JGK4 | Q0JGK4 |
| S-adenosyl-L-methionine biosynthesis | P93438 | | |
| L-homocysteine biosynthesis | Q84VE1 | | |
| urea degradation | E0ZS48 | | E0ZS48 |
| protoporphyrin-IX biosynthesis | Q10LR9 | | |
| tetrahydrofolate interconversion | Q7Y1F0;Q10BJ7 | Q7Y1F0 | Q10BJ7 |
| flavonoid biosynthesis | Q2R3A1 | | |
| glutathione biosynthesis | Q6Z3A3 | | Q6Z3A3 |
| pentose phosphate pathway | Q10M94 | | Q10M94 |
| Glycolysis | Q6K5G8;Q7XKB5;Q7FAH2;B8ACJ0 | Q6K5G8 | Q6K5G8 |
| AMP biosynthesis via de novo pathway | A2XD35 | | A2XD35 |
| isopentenyl diphosphate biosynthesis via DXP pathway | Q5N8G1 | | Q5N8G1 |
| chorismate biosynthesis | B8AKA5 | | B8AKA5 |

[a]PK1, booting stage; PK2, flowering stage; PK3, milk-ripe stage.

doi:10.1371/journal.pone.0133696.t002

**Table 3. Pathway analysis of differentially downregulated expressed proteins in the flowering and milk-ripe stages compared with the booting stage.**

| Pathway | Control (PK1)[a] | Downregulated (PK2)[a] | Downregulated (PK3)[a] |
|---|---|---|---|
| L-methionine biosynthesis via salvage pathway | F4MG97 | | F4MG97 |
| trans-cinnamate biosynthesis | Q0DZE3;B7EFQ4;Q6K6Q1 | Q0DZE3 | |
| chlorophyll biosynthesis (light-independent) | Q9SDJ2 | | Q9SDJ2 |
| chlorophyll biosynthesis | Q6ATS0;Q53RM0 | | Q6ATS0;Q53RM0 |
| Pyruvate fermentation to lactate | Q0E4Q5 | Q0E4Q5 | Q0E4Q5 |
| Oxylipin biosynthesis | A2XL22 | A2XL22 | |
| sucrose biosynthesis | Q0JGK4 | | |
| S-adenosyl-L-methionine biosynthesis | P93438 | P93438 | P93438 |
| L-homocysteine biosynthesis | Q84VE1 | Q84VE1 | Q84VE1 |
| urea degradation | E0ZS48 | | |
| protoporphyrin-IX biosynthesis | Q10LR9 | | Q10LR9 |
| tetrahydrofolate interconversion | Q7Y1F0;Q10BJ7 | | |
| flavonoid biosynthesis | Q2R3A1 | Q2R3A1 | Q2R3A1 |
| glutathione biosynthesis | Q6Z3A3 | | |
| pentose phosphate pathway | Q10M94 | | |
| Glycolysis | Q6K5G8;Q7XKB5;Q7FAH2;B8ACJ0 | | Q7XKB5;Q7FAH2;B8ACJ0 |
| AMP biosynthesis via de novo pathway | A2XD35 | | |
| isopentenyl diphosphate biosynthesis via DXP pathway | Q5N8G1 | | |
| chorismate biosynthesis | B8AKA5 | | |

[a]PK1, booting stage; PK2, flowering stage; PK3, milk-ripe stage.

doi:10.1371/journal.pone.0133696.t003

ammonia-lyase (B7EFQ4) in the trans-cinnamate biosynthesis pathway, and the probable sucrose-phosphate synthase (Q0JGK4) in the sucrose biosynthesis pathway in the flowering and milk-ripe stages were obviously higher than in the booting stage. Compared with the booting stage, L-lactate dehydrogenase (Q0E4Q5) in the pyruvate fermentation to lactate pathway, S-adenosylmethionine synthase 2 (SAM2; P93438) in the S-adenosyl-L-methionine biosynthesis pathway, adenosylhomocysteinase (Q84VE1) in the L-homocysteine biosynthesis pathway, and chalcone synthase 1 (CHS1; Q2R3A1) in flavonoid biosynthesis pathway were all downregulated in the flowering and milk-ripe stages. Three significantly differentially expressed proteins were found to be associated with chlorophyll biosynthesis pathways. The expression of magnesium-protoporphyrin IX monomethyl ester [oxidative] cyclase (Q9SDJ2) was significantly up-regulated in the flowering stage, and down-regulated in the milk-ripe stage. The two magnesium-chelatase subunits, ChlD (Q6ATS0) and ChlI (Q53RM0), were down-regulated in the milk-ripe stage (Table 3). Among these chlorophyll biosynthesis pathway related proteins, the expression of magnesium-protoporphyrin IX monomethyl ester [oxidative] cyclase (Q9SDJ2) in the flowering and milk-ripe stages was validated by qRT-PCR, while ChlD (Q6ATS0) and ChlI (Q53RM0) was validated down-regulated in the milk-ripe stage (Fig 5).

## Discussion

Knowledge of proteomic changes that occur during rice hull development is important for understanding the mechanism that determines rice yield and quality. Many genetic and genomic resources have been used to elucidate details of the molecular mechanisms of rice hull development; however, until now, this information has been limited to a small number of genes [8, 13, 15–17] and was based mainly on genomic techniques [39, 40]. As a result, only
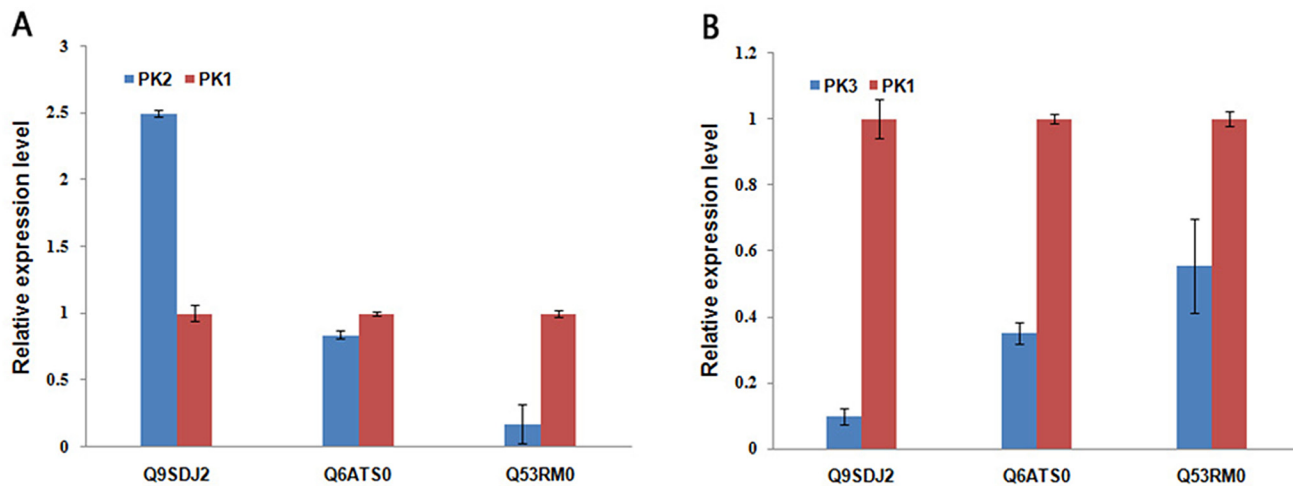
**Fig 5. Validation of differentially expressed proteins in chlorophyll biosynthesis pathways.** P1, booting stage; P2, flowering stage; P3, milk-ripe stage.

some biological characteristics of rice hull development have been investigated. The recent development of iTRAQ has allowed full-scale alterations of protein expression profiles to be examined under particular defined conditions [24–26, 41, 42]. To reduce the impact of individuals, we pooled rice hull samples from various development stages in the iTRAQ study. Our results showed that the label-based iTRAQ quantitative proteomic approach successfully detected and quantified the overall protein profile alternations in the booting, flowering, and milk-ripe stages of rice hull development. The unsupervised hierarchical clustering analysis indicated that the protein profiles of the flowering and milk-ripe stages were more similar to each other than they were to the protein profile of the booting stage (Fig 2A). When GO terms were assigned to the differentially expressed proteins in the three development stages, we found that the GO term numbers in the booting and flowering stages were more similar than either of them were to GO term numbers in the milk-ripe stage. This finding suggested that the level of activity in the rice hull proteome was similar in the booting and flowering stages compared with in the milk-ripe stage. The overall gene ontology analysis showed that GO terms of biological process and cellular component were much more diverse than molecular function terms in three growth stages of rice hull. It indicated that molecular function terms would be more likely to distinguish the characterization of rice hull at various growth stages.

Molecular function was highlighted to help understand the protein activities at the molecular level. Nine GO terms under the molecular function category were enriched and differentially overexpressed at various growth stages. We identified 25 candidate proteins annotated with five GO terms; two for oxidoreductase activity (GO:0016620 and GO:0016903), the others for transaminase activity (GO:0008483), transferase activity (GO:0016769), and flavin adenine dinucleotide binding (GO:0050660). The unannotated protein (Q7X8A1) was overexpressed especially in the flowering stage, indicating that this protein may be an important regulatory protein that distinguishes the flowering stage from the other growth stages. A putative uncharacterized protein (B8BF94) and ALDH (Q9FPK6) were overexpressed only in the milk-ripe stage, suggesting that these proteins may be crucial in the milk-ripe stage of rice hull development. Some proteins, for example, GAPC3 (Q6K5G8) and Aldh2b (Q9FRX7), were overexpressed in the flowering and milk-ripe stages, indicating that they may play pivotal roles in these two growth stages. The 25 identified candidate proteins may be major contributors to the heterogeneity of the rice hull proteome at various growth stages.

Pathways regulated by differentially expressed proteins offered an opportunity to observe the dynamic cell behavior in the rice hull development. In each cell, signal transduction and regulatory systems transmit information from the cell to its environmental status, thereby controlling the expression levels of every protein in the cell. UniPathway [38], a manually curated pathway database, was used to analyze the biology mechanisms of the differentially expressed proteins in the proteomic analysis to determine the dynamic cell behavior during rice hull development. GAPC3 (Q6K5G8) was upregulated in the glycolysis pathway in the flowering and milk-ripe stages compared with in the booting stage. Glycolysis is a pivotal process in the breakdown of glucose to generate energy and to provide biosynthetic precursors for cellular materials [43]. Glycolysis also plays an important role in maintaining cell division and controlling cell proliferation [44, 45]. The high expression of GAPC3 in the flowering and milk-ripe stages suggested that this protein may play a pivotal role in the glycolysis pathway during rice hull development. Sucrose metabolism is known to play crucial roles in development, stress response, and yield formation [46]. Deficient sucrose has been reported to cause an overall decrease in cell wall polymers [47]. A probable sucrose-phosphate synthase (Q0JGK4) was upregulated in the flowering and milk-ripe stages, suggesting that it might be an important regulator in sucrose biosynthesis. Other pathways such as light-dependent chlorophyll biosynthesis and oxylipin biosynthesis were also found to be related to rice hull development. Chlorophyll biosynthesis plays essential roles in photosynthesis [48], and oxylipin biosynthesis plays important roles in adaptation to photo-oxidative stress [49]. The rice grain thickens and hardens during the milk-ripe stage and, at the same time, the outer covering changes from green to yellow. Upregulation of the magnesium-protoporphyrin IX monomethyl ester [oxidative] cyclase (Q9SDJ2) in the flowering stage suggested that it may be involved in chlorophyll accumulation and chloroplast development. Three chlorophyll biosynthesis pathways related proteins involved to magnesium-protoporphyrin IX monomethyl ester [oxidative] cyclase (Q9SDJ2), ChID (Q6ATS0) and Ch1I (Q53RM0), were significantly downregulated in the milk-ripe stage. These proteins, especially magnesium-protoporphyrin IX monomethyl ester [oxidative] cyclase (Q9SDJ2) identified by qRT-PCR, may directly influence the biosynthesis of chlorophyll and eventually change the chlorophyll content at the different developmental stages. To our knowledge, this is the first study to use the well established quantitative iTRAQ label-based technology for proteomic analysis of rice hull during its development. We identified 25 differentially expressed proteins that may be associated with various growth stages. GO terms and pathways with related protein expression alterations may provide new insights into the mechanisms of rice hull development. The results have provided new information for understanding the molecular characterization of rice hull development at various growth stages.

## Conclusions

This study provides a global profiling of changes in the rice hull proteome during development. GO and pathways analysis of the differentially expressed proteins revealed dynamic cell behavior during hull development, and provided new insights into the molecular mechanisms of rice hull development at various growth stages.

## Supporting Information

**S1 Fig. Cellular function analysis of differentially expressed proteins in three growth stages of rice hull.** P1, booting stage; P2, flowering stage; P3, milk-ripe stage
(GIF)

**S2 Fig. Biological process analysis of differentially expressed proteins in three growth stages of rice hull.** P1, booting stage; P2, flowering stage; P3, milk-ripe stage.
(GIF)

**S1 Table. Quantitative changes of differentially expressed proteins in rice hulls at various growth stages.**
(XLS)

**S2 Table. GO classification of differentially expressed proteins involved in booting stage (PK1), flowering stage (PK2) and milk-ripe stage (PK3).**
(XLS)

## Acknowledgments

## Author Contributions

Conceived and designed the experiments: SLR HSM. Performed the experiments: SZW WYC WFX CDY YX JRQ WMH YPF JXT GCH ZZC WY. Analyzed the data: ZZC XPF HY WGL. Contributed reagents/materials/analysis tools: SZW WYC WFX WY. Wrote the paper: SZW.

## References

1. Guo S-b, Wei Y, Li X-q, Liu K-q, Huang F-k, Chen C-h, et al. (2013) Development and Identification of Introgression Lines from Cross of Oryza sativa and Oryza minuta. Rice Science 20: 95–102.

2. Lu C, Liu J, Jiang J-h, BRERIA CM, Tan H-l, ICHII M, et al. (2013) Development and Application of SCAR Markers for Discriminating Cytoplasmic Male Sterile Lines from Their Cognate Maintainer Lines in Indica Rice. Rice Science 20: 191–199.

3. Normile D (2008) Agricultural research. Reinventing rice to feed the world. Science 321: 330–333. doi: 10.1126/science.321.5887.330 PMID: 18635770

4. Sasaya T, Nakazono-Nagaoka E, Saika H, Aoki H, Hiraguri A, Netsu O, et al. (2014) Transgenic strategies to confer resistance against viruses in rice plants. Front Microbiol 4: 409. doi: 10.3389/fmicb.2013.00409 PMID: 24454308

5. Taiz L and Zeiger E (2012) Plant Physiology, Third Edition. Sinauer Associates, Sunderland, MA: 484.

6. Yu X-r, Zhou L, Xiong F, Wang Z (2014) Structural and Histochemical Characterization of Developing Rice Caryopsis. Rice Science 21: 142–149.

7. Fan C, Xing Y, Mao H, Lu T, Han B, Xu C, et al. (2006) GS3, a major QTL for grain length and weight and minor QTL for grain width and thickness in rice, encodes a putative transmembrane protein. Theor Appl Genet 112: 1164–1171. PMID: 16453132

8. Li X, Sun L, Tan L, Liu F, Zhu Z, Fu Y, et al. (2012) TH1, a DUF640 domain-like gene controls lemma and palea development in rice. Plant Mol Biol 78: 351–359. doi: 10.1007/s11103-011-9868-8 PMID: 22203474

9. Luo L-l, Zhang Y-x, Chen D-b, Zhan X-d, Shen X-h, Cheng S-h, et al. (2014) QTL Mapping for Hull Thickness and Related Traits in Hybrid Rice Xieyou 9308. Rice Science 21: Pages 29–38.

10. Shomura A, Izawa T, Ebana K, Ebitani T, Kanegae H, Konishi S, et al. (2008) Deletion in a gene associated with grain size increased yields during rice domestication. Nat Genet 40: 1023–1028. doi: 10.1038/ng.169 PMID: 18604208

11. Song XJ, Huang W, Shi M, Zhu MZ and Lin HX (2007) A QTL for rice grain width and weight encodes a previously unknown RING-type E3 ubiquitin ligase. Nat Genet 39: 623–630. PMID: 17417637

12. Weng J, Gu S, Wan X, Gao H, Guo T, Su N, et al. (2008) Isolation and initial characterization of GW5, a major QTL associated with rice grain width and weight. Cell Res 18: 1199–1209. doi: 10.1038/cr.2008. 307 PMID: 19015668

13. Li J-b, Xia M-y, Wan B-l, Du X-s, Zha Z-p, Yu D-z, et al. (2009) Genetic Analysis and Mapping of TWH Gene in Rice Twisted Hull Mutant. Rice Science 16: 79–82.

14. Wei X, Zhang X, Shao G, He J, Jiao G, Xie L, et al. (2013) Fine mapping of BH1, a gene controlling lemma and palea development in rice. Plant cell reports 32: 1455–1463. doi: 10.1007/s00299-013-1457-7 PMID: 23689259

15. Wang SS, Wang CS, Tseng TH, Hou YL and Chen KY (2011) High-resolution genetic mapping and candidate gene identification of the SLP1 locus that controls glume development in rice. Theor Appl Genet 122: 1489–1496. doi: 10.1007/s00122-011-1548-1 PMID: 21327937

16. Jin Y, Luo Q, Tong H, Wang A, Cheng Z, Tang J, et al. (2011) An AT-hook gene is required for palea formation and floral organ number control in rice. Dev Biol 359: 277–288. doi: 10.1016/j.ydbio.2011.08. 023 PMID: 21924254

17. Prasad K, Parameswaran S, Vijayraghavan U (2005) OsMADS1, a rice MADS-box factor, controls differentiation of specific cell types in the lemma and palea and is an early-acting regulator of inner floral organs. Plant J 43: 915–928. PMID: 16146529

18. Komatsu M, Chujo A, Nagato Y, Shimamoto K, Kyozuka J (2003) FRIZZY PANICLE is required to prevent the formation of axillary meristems and to establish floral meristem identity in rice spikelets. Development 130: 3841–3850. PMID: 12835399

19. Zhang Q, Xu J, Li Y, Xu P, Zhang H, Wu X (2007) Morphological, anatomical and genetic analysis for a rice mutant with abnormal hull. Journal of genetics and genomics = Yi chuan xue bao 34: 519–526. PMID: 17601611

20. Yoshida A, Suzaki T, Tanaka W, Hirano HY (2009) The homeotic gene long sterile lemma (G1) specifies sterile lemma identity in the rice spikelet. Proceedings of the National Academy of Sciences of the United States of America 106: 20103–20108. doi: 10.1073/pnas.0907896106 PMID: 19901325

21. Hong L, Qian Q, Zhu K, Tang D, Huang Z, Gao L, et al. (2010) ELE restrains empty glumes from developing into lemmas. Journal of genetics and genomics = Yi chuan xue bao 37: 101–115. doi: 10.1016/S1673-8527(09)60029-1 PMID: 20227044

22. Cao P, Jung KH, Choi D, Hwang D, Zhu J, Ronald PC (2012) The Rice Oligonucleotide Array Database: an atlas of rice gene expression. Rice (N Y) 5: 17.

23. Deswal R, Gupta R, Dogra V, Singh R, Abat JK, Sarkar A, et al. (2013) Plant proteomics in India and Nepal: current status and challenges ahead. Physiology and molecular biology of plants: an international journal of functional plant biology 19: 461–477.

24. Ghosh D, Li Z, Tan XF, Lim TK, Mao Y, Lin Q (2013) iTRAQ based quantitative proteomics approach validated the role of calcyclin binding protein (CacyBP) in promoting colorectal cancer metastasis. Mol Cell Proteomics 12: 1865–1880. doi: 10.1074/mcp.M112.023085 PMID: 23543800

25. Huang X, Zeng Y, Xing X, Zeng J, Gao Y, Cai Z, et al. (2014) Quantitative proteomics analysis of early recurrence/metastasis of huge hepatocellular carcinoma following radical resection. Proteome Sci 12: 22. doi: 10.1186/1477-5956-12-22 PMID: 24839399

26. Kambiranda D, Katam R, Basha SM, Siebert S (2014) iTRAQ-based quantitative proteomics of developing and ripening muscadine grape berry. J Proteome Res 13: 555–569. doi: 10.1021/pr400731p PMID: 24251720

27. Latterich M, Abramovitz M, Leyland-Jones B (2008) Proteomics: new technologies and clinical applications. Eur J Cancer 44: 2737–2741. doi: 10.1016/j.ejca.2008.09.007 PMID: 18977654

28. Wilm M (2009) Quantitative proteomics in biological research. Proteomics 9: 4590–4605. doi: 10.1002/pmic.200900299 PMID: 19743428

29. Wisniewski JR, Zougman A, Nagaraj N, Mann M (2009) Universal sample preparation method for proteome analysis. Nat Methods 6: 359–362. doi: 10.1038/nmeth.1322 PMID: 19377485

30. Shilov IV, Seymour SL, Patel AA, Loboda A, Tang WH, Keating SP, et al. (2007) The Paragon Algorithm, a next generation search engine that uses sequence temperature values and feature probabilities to identify peptides from tandem mass spectra. Mol Cell Proteomics 6: 1638–1655. PMID: 17533153

31. Gentleman RC, Carey VJ, Bates DM, Bolstad B, Dettling M, Dudoit S, et al. (2004) Bioconductor: open software development for computational biology and bioinformatics. Genome Biol 5: R80. PMID: 15461798

32. Blake JA, Dolan M, Drabkin H, Hill DP, Li N, Sitnikov D, et al. (2013) Gene Ontology annotations and resources. Nucleic Acids Res 41: D530–535. doi: 10.1093/nar/gks1050 PMID: 23161678

33. UniProt (2013) Update on activities at the Universal Protein Resource (UniProt) in 2013. Nucleic Acids Res 41: D43–47. doi: 10.1093/nar/gks1068 PMID: 23161681

34. Zheng Q, Wang XJ (2008) GOEAST: a web-based software toolkit for Gene Ontology enrichment analysis. Nucleic Acids Res 36: W358–363. doi: 10.1093/nar/gkn276 PMID: 18487275

35. Sakai H, Lee SS, Tanaka T, Numa H, Kim J, Kawahara Y, et al. (2013) Rice Annotation Project Database (RAP-DB): an integrative and interactive database for rice genomics. Plant & cell physiology 54: e6.

36. Ouyang S, Zhu W, Hamilton J, Lin H, Campbell M, Childs K, et al. (2007) The TIGR Rice Genome Annotation Resource: improvements and new features. Nucleic Acids Res 35: D883–887. PMID: 17145706

37. Krzywinski M, Schein J, Birol I, Connors J, Gascoyne R, Horsman D, et al. (2009) Circos: an information aesthetic for comparative genomics. Genome Res 19: 1639–1645. doi: 10.1101/gr.092759.109 PMID: 19541911

38. Morgat A, Coissac E, Coudert E, Axelsen KB, Keller G, Bairoch A, et al. (2012) UniPathway: a resource for the exploration and annotation of metabolic pathways. Nucleic Acids Res 40: D761–769. doi: 10.1093/nar/gkr1023 PMID: 22102589

39. Ashikari M, Matsuoka M (2006) Identification, isolation and pyramiding of quantitative trait loci for rice breeding. Trends in plant science 11: 344–350. PMID: 16769240

40. Huang R, Jiang L, Zheng J, Wang T, Wang H, Huang Y, et al. (2013) Genetic bases of rice grain shape: so many genes, so little known. Trends in plant science 18: 218–226. doi: 10.1016/j.tplants.2012.11.001 PMID: 23218902

41. Liu GT, Ma L, Duan W, Wang BC, Li JH, Xu HG, et al. (2014) Differential proteomic analysis of grapevine leaves by iTRAQ reveals responses to heat stress and subsequent recovery. BMC plant biology 14: 110. doi: 10.1186/1471-2229-14-110 PMID: 24774513

42. Poulsen ET, Dyrlund TF, Runager K, Scavenius C, Krogager TP, Hojrup P, et al. (2014) Proteomics of Fuchs' Endothelial Corneal Dystrophy support that the extracellular matrix of Descemet's membrane is disordered. J Proteome Res.

43. Mulukutla BC, Yongky A, Daoutidis P, Hu WS (2014) Bistability in glycolysis pathway as a physiological switch in energy metabolism. PloS one 9: e98756. doi: 10.1371/journal.pone.0098756 PMID: 24911170

44. Monahan LG, Hajduk IV, Blaber SP, Charles IG, Harry EJ (2014) Coordinating bacterial cell division with nutrient availability: a role for glycolysis. mBio 5: e00935–00914. doi: 10.1128/mBio.00935-14 PMID: 24825009

45. TeSlaa T, Teitell MA (2014) Techniques to monitor glycolysis. Methods in enzymology 542: 91–114. doi: 10.1016/B978-0-12-416618-9.00005-4 PMID: 24862262

46. Ruan YL (2014) Sucrose metabolism: gateway to diverse carbon use and sugar signaling. Annual review of plant biology 65: 33–67. doi: 10.1146/annurev-arplant-050213-040251 PMID: 24579990

47. Gerber L, Zhang B, Roach M, Rende U, Gorzsas A, Kumar M, et al. (2014) Deficient sucrose synthase activity in developing wood does not specifically affect cellulose biosynthesis, but causes an overall decrease in cell wall polymers. The New phytologist.

48. Chen M (2014) Chlorophyll modifications and their spectral extension in oxygenic photosynthesis. Annual review of biochemistry 83: 317–340. doi: 10.1146/annurev-biochem-072711-162943 PMID: 24635479

49. Satoh M, Tokaji Y, Nagano AJ, Hara-Nishimura I, Hayashi M, Nishimura M, et al. (2013) Arabidopsis mutants affecting oxylipin signaling in photo-oxidative stress responses. Plant physiology and biochemistry: PPB / Societe francaise de physiologie vegetale.